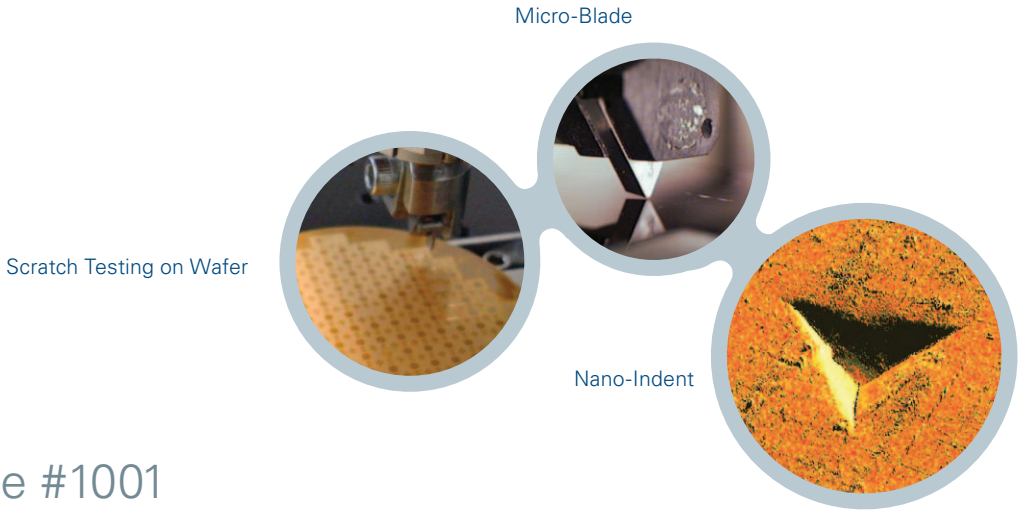

Application Note #1001

Thin Film and Coating Testing Using Bruker's UMT Testers

New thin films and coatings are being deployed in a wide variety of applications for semiconductors, displays, solar panels and LEDs, to name just a few. While bulk material properties can be determined using any number of established techniques, measuring material properties of thin films in-situ requires instrumented analysis. Latest advances in nano and micro tribology have led to the development of integrated instrumentation utilizing simultaneous measurements of normal load, friction force, contact acoustic emission and electrical resistance. Instruments with this advanced functionality can perform common mechanical tests, such as indentation, scratch, and reciprocating wear, while on the same platform to enable very sensitive detailed imaging of the coatings through integrated atomic-force microscopy or optical microscopy. This note discusses how the use of this instrumentation in the study of mechanical properties of thin films and coatings has resulted in a number of interesting applications.

Experimental Applications

Nanoindentation for Optoelectronics

Multiphase and porous ceramic materials are being used as passive semiconductors for building modern optoelectronic devices. Prescreening critical parts for subsurface defects before assembly can prevent potential device failures in the field. A new nanoindentation-based method has been proposed where shapes of loading–unloading curves can fingerprint subsurface cracking and material porosity-induced inelastic behavior in defected multiphase ceramic parts (see Figure 1).

Three typical experimental curve types can be distinguished in describing nanoscale contact behavior of multiphase porous low-k ceramics. The Type I curve shape can be attributed to the normal loading-unloading situation, where cracks are not observed. Type II can be attributed to the case of a cracked contact, where large excursions can be observed on the loading segment of the curve; there, a large resultant displacement produced a low hardness value. Type III load–unload curve shape can be associated with the inelastic behavior, where the shell bending effect during indenting into the void can be observed.

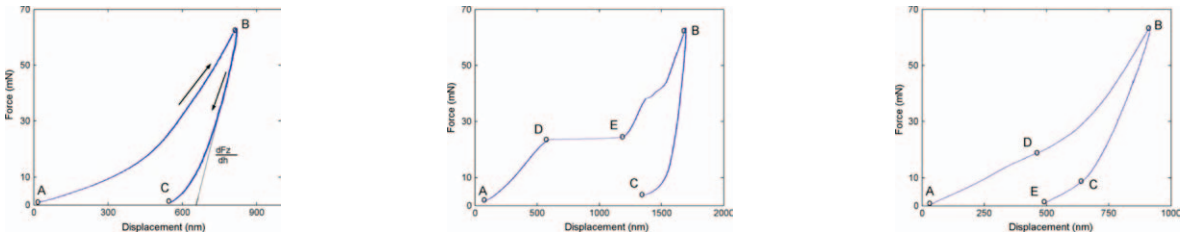

Figure 1. Shape of loading-unloading curves: Type I (a) for normal nanoindentation, Type II (b) corresponding to the crack, and Type III (c) corresponding to the inelastic response and can be attributed to the air bubble beneath the surface.

Measured elastic modulus (Er), nanohardness (H) and Knoop hardness (HK) values were obtained for every sample, at three locations (#1, #2, #3). Experimental data suggest that the observed scattering of H and HK is a result of the non-homogeneity of the low-K material, due to the presence of multiple phases. It is observed that in the cracked or void-filled areas nanohardness is two to four times lower than values measured at other locations. A very consistent result trend, obtained from the destructive microhardness Knoop tests, verified the findings. Contact stiffness and resulting E_r had large errors due to the non-homogeneity of samples as well as rough surfaces. Nanoindentation instrument errors were negligible for the applied 30–70mN loads.

Scratch-Hardness Test of Hard Coatings

Micro-scratch-hardness tests were performed on two specimens using a diamond stylus with a tip radius of 5µm. The test was conducted with reference to ASTM G171-03 (Standard Test Method for Scratch Hardness of Materials Using a Diamond Stylus), modified for thin coatings. The scratch hardness of a material can be determined by producing a scratch on the sample surface with a sharp, hard (diamond) tool with known tip geometry, under a constant, load. Measuring the scratch width, one can define the sample scratch hardness as:

$$HSp = k * Fz / W^2$$

where HSp is the scratch hardness number, k is a constant, Fz is applied load, and W is scratch width.

When the constant k is unknown, the scratch hardness can be determined by comparison of the scratch width on the sample and on a reference material with known hardness value:

$$HS_{sample} = (HS_{ref} * W_{ref}^{\ 2} / Fz_{ref}) * Fz_{sample} / W_{sample}^{\ 2}$$

where the indices "sample" and "ref" refer to the test sample and reference material, respectively.

The diamond stylus in a stylus holder was mounted on the force sensor with a spring suspension. The test sample was mounted on a table of the lower linear drive, allowing for automated lateral motion and thereby multiple scratches on a single specimen. An acoustic emission sensor was attached to the stylus holder to monitor the high-frequency signal generated during scratching, which indicates the intensity of material fracture.

To begin the test, a normal load of 0.4N was applied to the stylus. The scratch was produced by dragging the stylus along the sample surface with the upper lateral slider. The scratch length was 5mm, and dragging speed was 0.5mm/s. Load was maintained constant throughout the test by controlling the z-carriage motion based on closed-loop feedback from the force gauge.

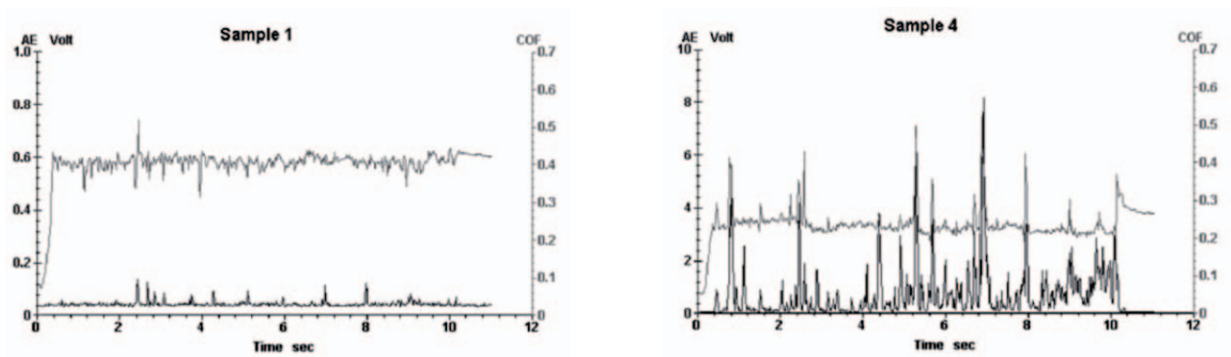

Figure 2. Friction coefficient (gray) and AE (black) signals during micro-scratch tests on samples 1 and 4.

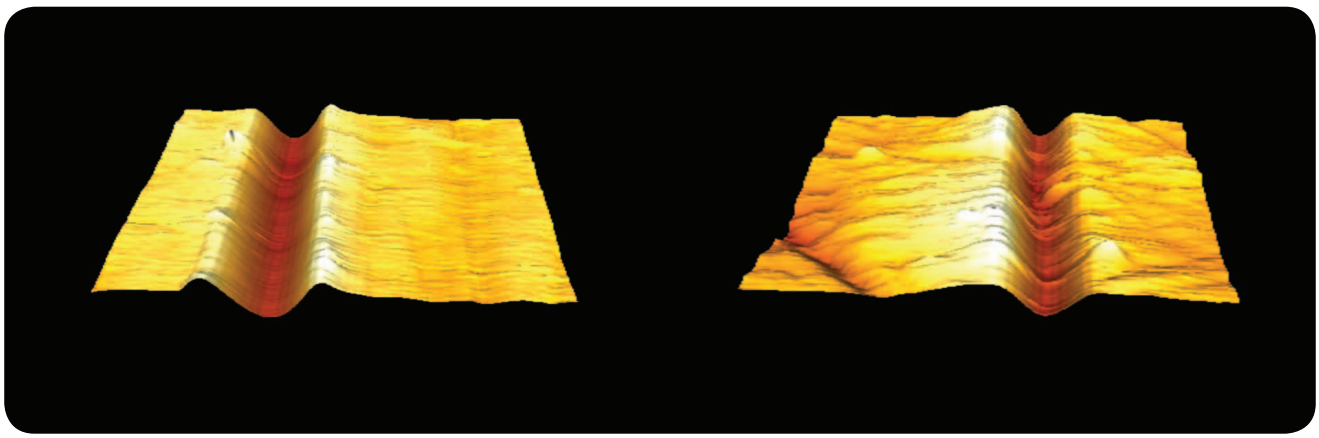

Figure 3. 3D AFM images of scratches on sample 1 (a) and sample 2 (b) at a scan size of 25µm x 25µm.

The test was repeated three times on each sample to verify the data consistency and repeatability. A polished fused quartz (with the hardness of 9.5GPa) was used as the reference material for the scratch-hardness calculations. COF and AE data as a function of time are plotted in Figure 2.

Following the test, the scratch width was measured by an atomic force microscope (AFM) head, and AFM images of the scratches were taken. Table 1 shows the mean values of the coefficient of friction (COF) and acoustic emission (AE) for both specimens, along with the scratch width W and scratch hardness. Figure 3 shows 3D AFM images of the scratches on both samples. Screenshots with the scratch width measurements are shown in Figure 4.

Table 1. Micro-scratch test data with diamond stylus.

Sample #	Mean COF	Mean AE	W, µm	HS, GPa
1	0.49	0.04	5.87	23.40
4	0.27	0.67	5.00	32.20

Scratch-Adhesion on LCD Display Samples

Conceptually similar to scratch-hardness, scratch adhesion with a micro-indenter or a micro-blade is performed by sliding under a linearly increasing load (Fz). The failure of the coating is characterized by sudden change in coefficient of friction (COF) or contact acoustic emission (AE). Adhesion strength of the coating or thin film is characterized by the corresponding load at which COF and AE exhibit a sudden change.

Figure 5 shows data from scratch-adhesion tests using a diamond stylus with a 12.5µm tip radius, at a sliding speed of 0.5mm/s over a distance of 10mm on a patterned LCD display with a coating layer sequence of indium-tin-oxide/overcoat/matrix on a glass substrate. At the point of failure at load of about 16mN, both COF and AE increased. The periodic bumps in the COF and Fz plot were due to the rapid interaction of the diamond tip with the patterned top surface of the specimen.

During the test, the indenter moved slowly on the coating, causing some material removal (Figure 6). A series of runs with progressively increasing normal loads, though constant within each run, was performed. The normal load started from 1N in the first run and was increased by 0.5N each run until coating failure was observed. The critical load characterizing the coating scratch resistance was defined as the minimum load to cut through the coating completely.

The results for three different LCD samples, each tested three times (see Table 2), show repeatable differences between coatings. The typical scratch raw data are presented in Figure 7 and Figure 8, illustrating various stages in the process of cutting through the coatings with the load increase.

Table 2. Scratch Test Results

Sample ID	Critical Load (N)		
	1st Test	2nd Test	3rd Test
1	5.0	5.5	5.5
2	4.0	4.0	4.0
3	2.5	3.0	2.5

In wear testing, the indenter was stationary, while the sample stage was reciprocating, which caused coating wear. Having determined the critical load required for coating failure in the scratch test above, a constant load of 1N was chosen for the wear test. The goal was to determine a load that would stress the material but not break through immediately. Following application of the load, the sample was cycled in a reciprocating motion until the coating was worn through. Coating wear resistance was defined as the minimum number of cycles to wear through the coating completely. The results for three different LCD samples, each tested three times and summarized in Table 3, show repeatable differences between the coatings. These results correlate with the scratch data in that the samples showing highest resistance to break through also show highest resistance to wear.

Table 3. Wear Test Results

Sample ID	Critical # Cycles, Thousands		
	1st Test	2nd Test	3rd Test
1	2.7	2.5	2.6
2	2.1	2.2	2.0
3	1.1	1.2	1.1

Tribological Properties of DLC Films

It is well known that the wear-resistance of monolithic materials can be greatly increased by the introduction of diamond-like carbon (DLC) thin films. Recently, DLC thin films have been used successfully in components such as rigid discs and microelectronic-mechanical systems (MEMS), whose protective coatings are required to have excellent wear-resistance in light load and high velocity working conditions. Tests were conducted to measure the variation of the frictional coefficients over time for an Al_2O_3 ball against a Si substrate (Figure 10a.). The test was repeated with a similar setup but, in this second case, the Si substrate was coated with a DLC film, approx. 250nm thick (Figure 10b.). The bare Si substrate sliding against the Al_2O_3 ball shows a frictional coefficient as high as 0.40–0.60. During the test wear, debris was visible to the naked eye after just a few sliding cycles, which indicated that the Si substrate has poor wear resistance. In contrast, the DLC film shows a much lower steady-state frictional coefficient of 0.13, and this remains almost unchanged even after two hours under the same test conditions.

Clearly the addition of a DLC film to the Si substrate greatly improves the wear resistance, and these tests provide invaluable data in evaluating the benefit of such friction-modifying coatings and in determining the relative performance improvements one could expect to see between different coating types. The coated material far outperforms the monolithic Si material, which makes it possible to use the DLC film as a promising protective coating to Si- and SiC-based components in MEMS.[6]

Mechanical and Tribological Properties of Carbon Nanotube (CNT) Composite Coatings

A steel ball is placed on top of the coated specimen with a normal load of 0.5–4 N. The coated specimen reciprocates underneath the ball at 3.0–5.0Hz. All the friction and wear tests were performed under unlubricated condition at room temperature and in ambient air

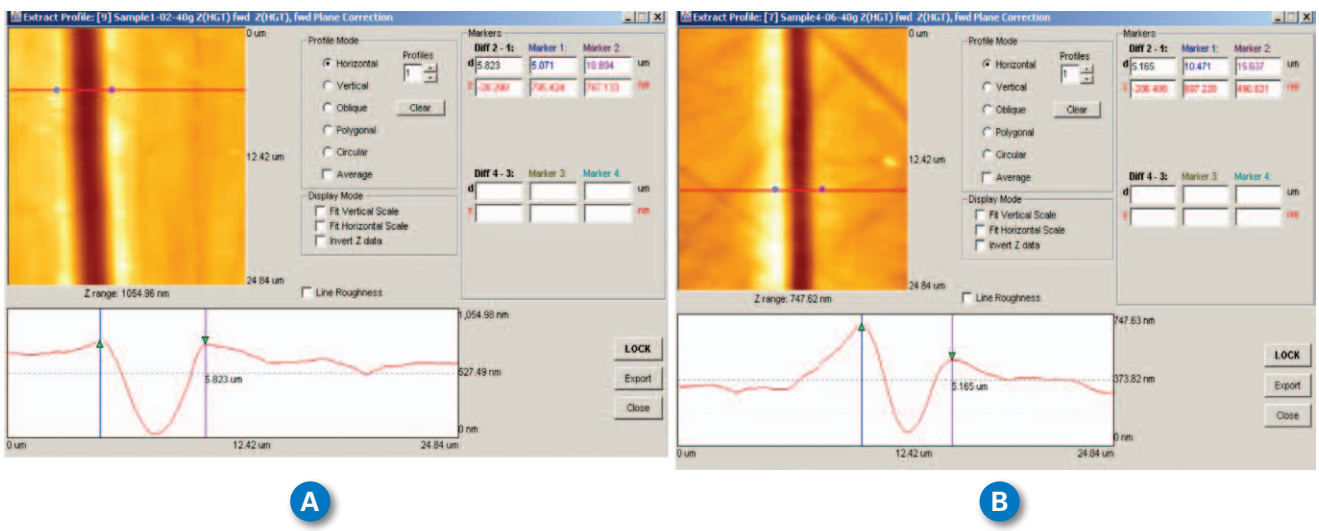

Figure 4. Example of scratch width measurement for sample 1 (a) and sample 4 (b).

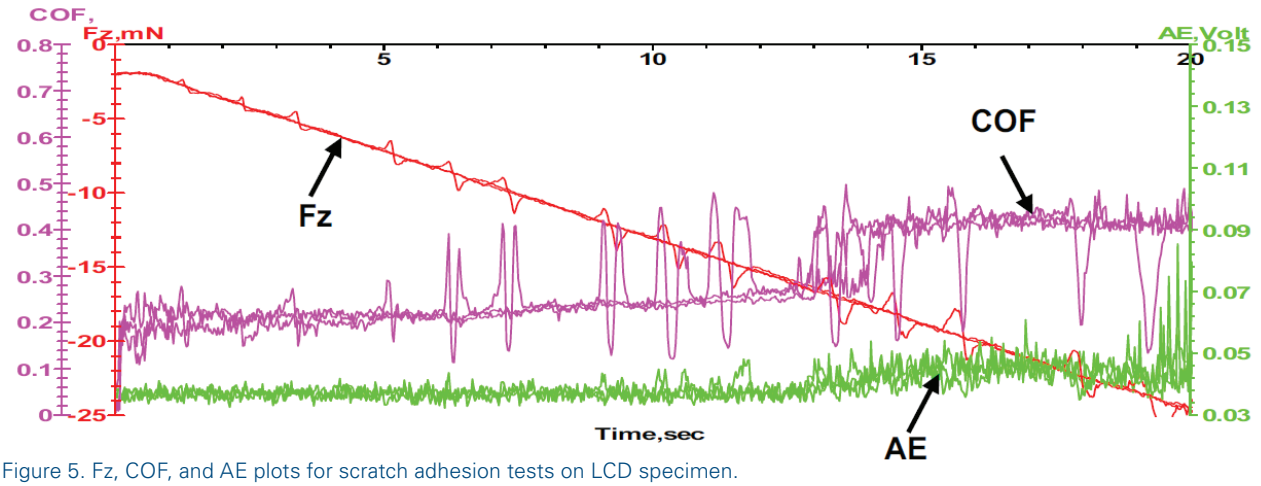

Figure 5. Fz, COF, and AE plots for scratch adhesion tests on LCD specimen.

(relative humidity 52%–56%). The friction coefficient was recorded continuously during the tests.

Figure 12 shows the typical load-unload curves for the Ni-Co and Ni-Co-CNTs composite coating subject to the nanoindentation measurement at a depth of 200nm. Based on the load-unload curves, the Ni-Co-CNTs composite coating had a nanoindentation hardness of 5.87GPa and an elastic modulus of 236GPa. The values for the Ni-Co alloy coating were 4.41GPa and 202GPa. This implies that the Ni-Co-CNTs composite coatings could have better tribological properties than the Ni-Co alloy coatings.[7]

Using the same basic test configuration, the friction coefficients for the Ni-Co coating and Ni-Co-CNTs composite coating were measured through multiple sliding cycles and the results are displayed in Figure 13. It is clear that the Ni-Co-CNTs composite coating has much lower friction coefficient than the Ni-Co alloy coating under the same test conditions, and the friction coefficient of each coating gradually increases over time under test.[7]

Another interesting observation is that the friction coefficient of the Ni-Co-CNTs composite coating decreases with increasing normal load under these test conditions. This could be attributed to the formation of a lubricious transfer layer on the counterpart surface during sliding. Subsequently, the friction is reduced owing to the formation of the lubricious transfer layer.[7]

Capabilities of Bruker Tribo-Testers

Based on the examples above, which are just a few of the known applications within the area of thin films and coatings testing, quite a number of tests can be carried out on Bruker's tribo-testers. This apparatus is a high-precision instrument for nano and micro mechanical testing of practically all types of thin films and coatings, including metals, ceramics, composites, polymers, etc.

The unique modular design permits the user to quickly reconfigure the instrument to any one of a number of test modes by simply swapping the easily-replaceable drive stages and sensors. A high-frequency multichannel data-acquisition system, with data sampling at thousands times per second, allows for detection of almost instantaneous tiny submicro-contact and submicro-failure events in sophisticated test sequences. Integrated optical microscopy is available for precision sample micro-positioning, digital video of the in-situ dynamics of surface failure and micro-images of wear tracks, indents and scratches. Optional integrated atomic force microscope and profilometry provide higher resolution imaging and quantification of test surfaces, wear tracks, indents and scratches, both periodically during testing and post-test.

Interchangeable Modules

Bruker tribo-testers have two easily-interchangeable modules (see Figure 14) that can accommodate either a nano-head or micro-head transducer-sensor assembly. Both heads can be used to measure hardness, Young's modulus, yield stress, fracture toughness, and contact

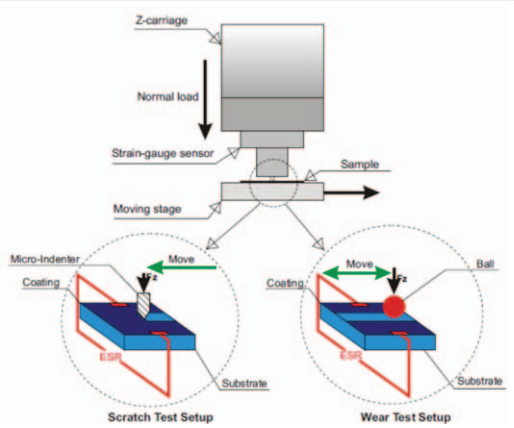

Figure 6. Schematic of scratch/wear test setups.

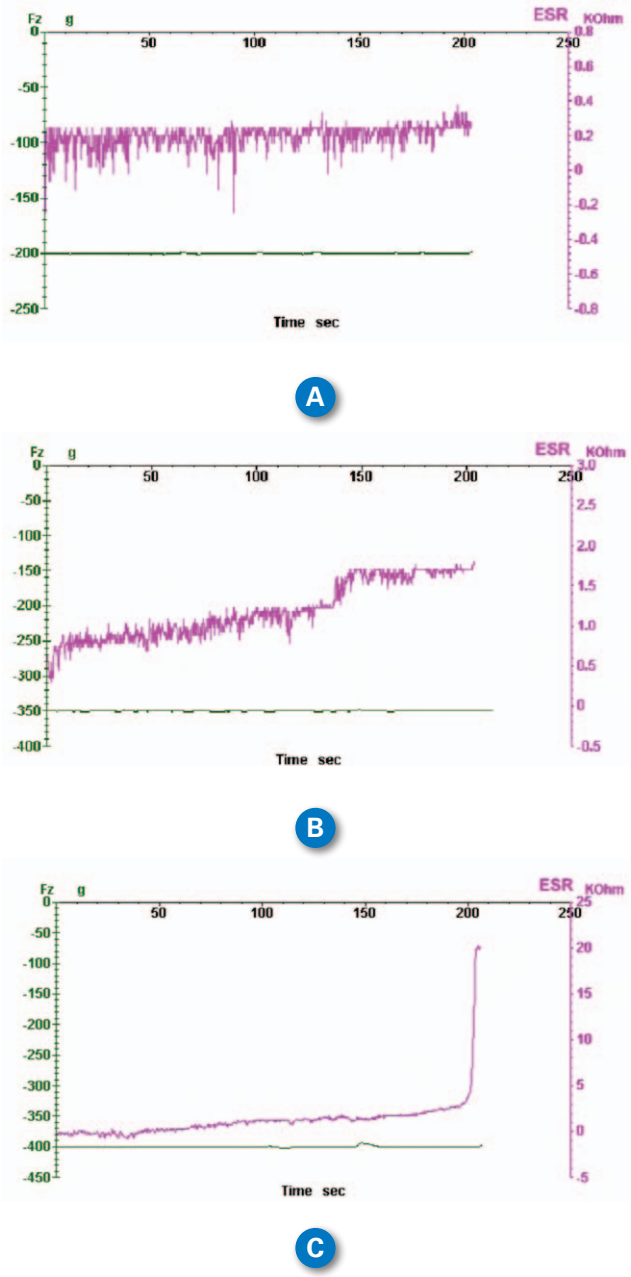

Figure 7. Sample 1: (a) at 2N the coating was not cut, (b) at 3.5N the coating started to break, (c) at 4N the coating broke, but did not totally cut through.

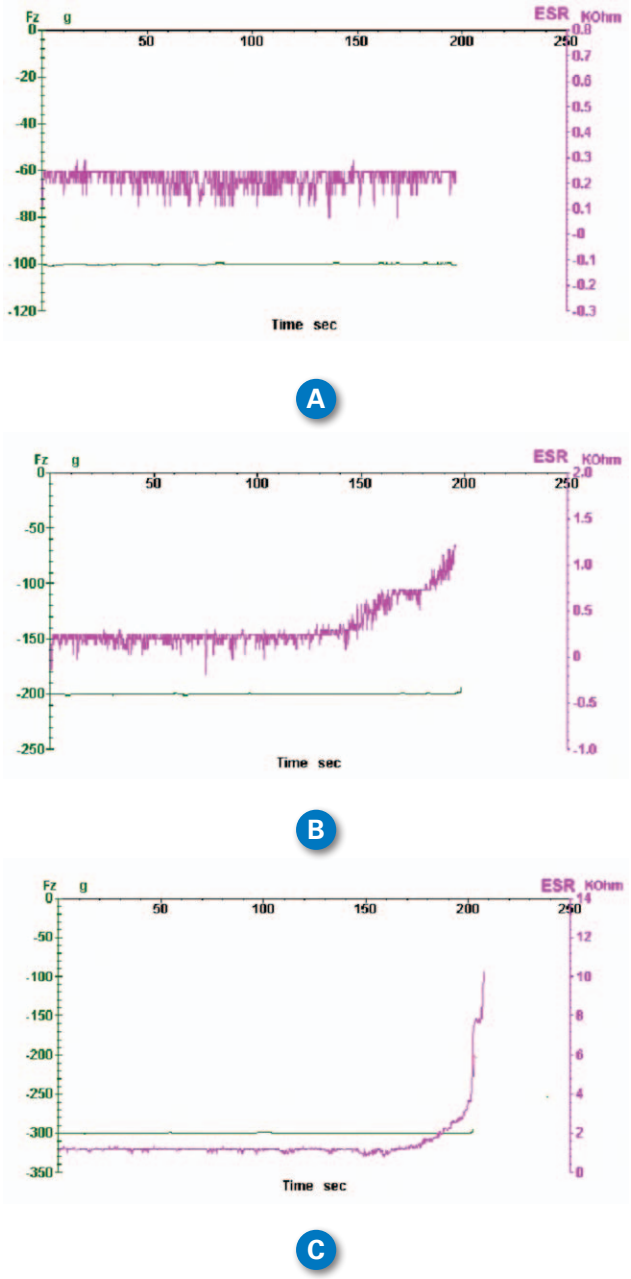

Figure 8. Sample 4: (a) at 1N the coating was not broken, (b) at 2N the coating started to break, (c) at 3N the coating broke, but did not totally cut through.

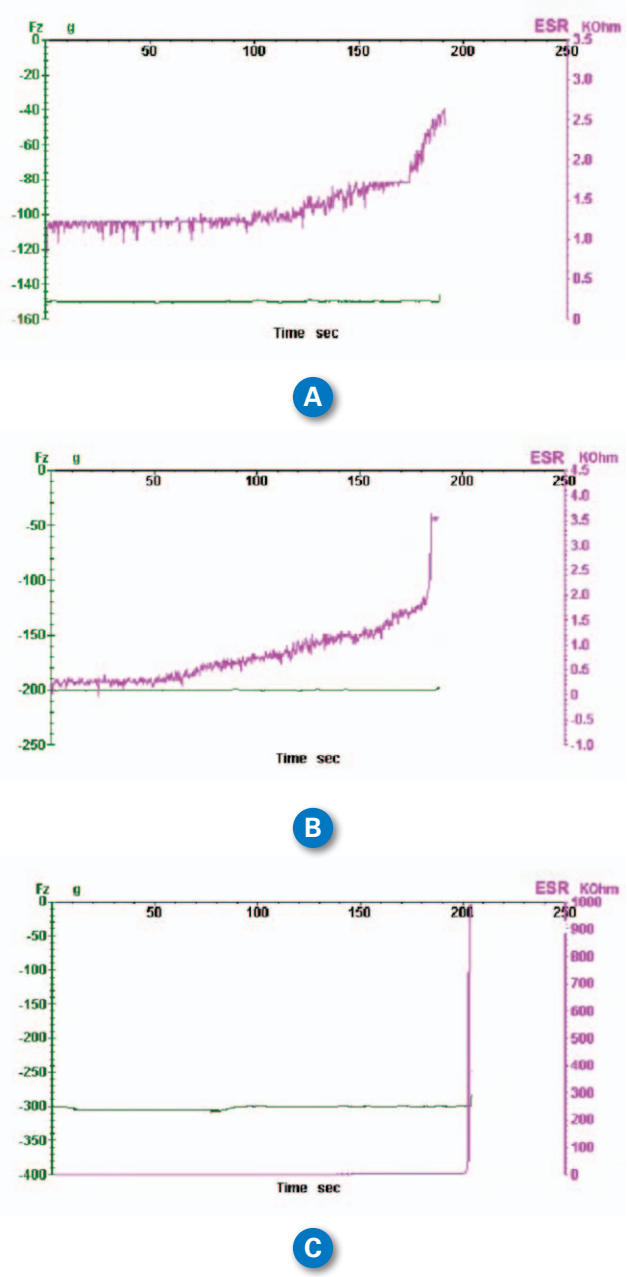

Figure 9. Sample 3: (a) at 1.5N the coating started to break, (b) at 2N coating broke, but did not totally cut through, (c) at 3N the coating was totally cut through.

stiffness or critical loads for onset of inelastic deformation during scratch and indentation tests. The nano-head is used primarily for thin films coatings and multi-phase materials, while the micro-head is used for bulk materials and relatively-thick films.

Both modules are equipped with an optical microscope and can also have an in-line imaging attachment, either AFM in the case of the nano-head or 3D profiler on the micro-head. The AFM measuring head contains a three-dimensional (3D) scanner with a probe holder and a laser-optic system for probe deflection detection, as well as an integrated digital optical microscope. Its scanning range is from 110x110x20µm. The 3D profiler measuring head contains a white light interferometer (WLI) x-y scanner with a stylus holder and a full-time color CCD camera. The 3D profiler's scanning range is from 10x10x10µm to 500x500x500µm.

Methodology for Scratch/Indentation Test

The following test procedure can be done on the Bruker tribo-testers for a comprehensive evaluation of the sample coatings/thin films properties:

- Nano/Micro-indentation tests for coating nano/micro-hardness and elastic modulus evaluation,
- Scratch-hardness tests under constant load for scratch resistance and hardness measurement,
- Scratch-adhesion tests under progressively increasing load for evaluation of the coating adhesion and scratch toughness properties,
- Slow reciprocating wear tests for evaluation of coating friction and durability.

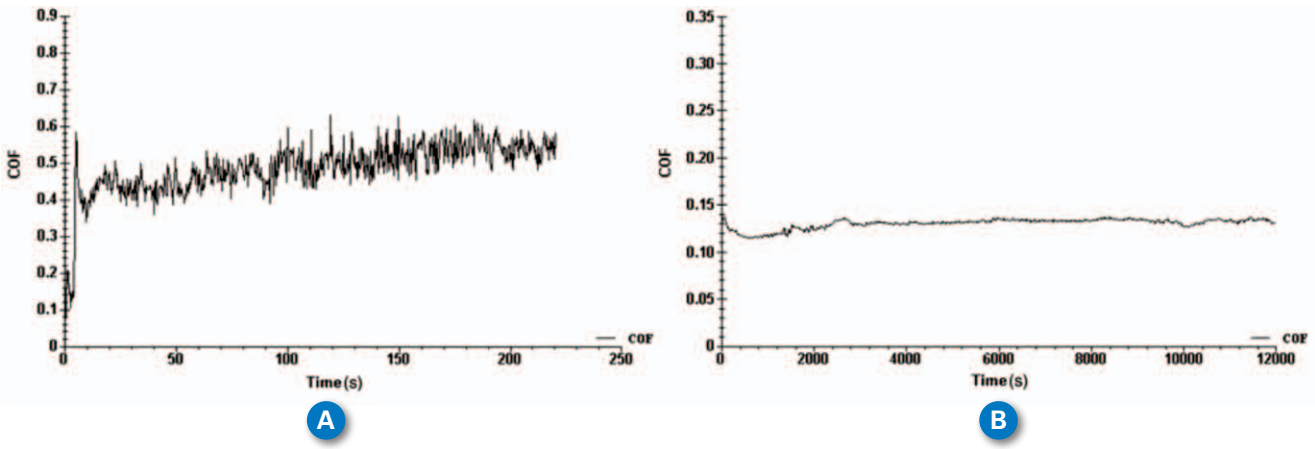

Figure 10. Variation of the friction coefficients with sliding time for (a) Si substrate against an Al_2O_3 ball and (b) DLC film about 250nm thick against the Al_2O_3 ball.

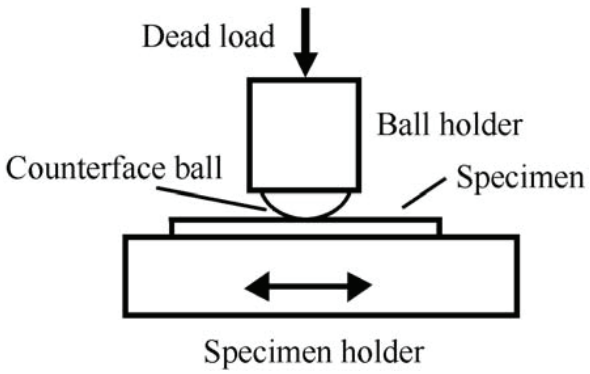

Figure 11. Contact configuration of the friction pair.

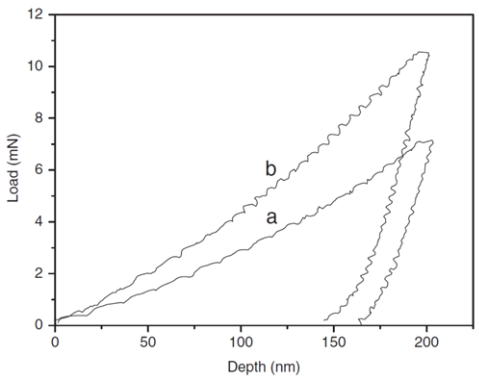

Figure 12. Typical load-displacement curves of(a) Ni-Co-CNTs composite coatings.

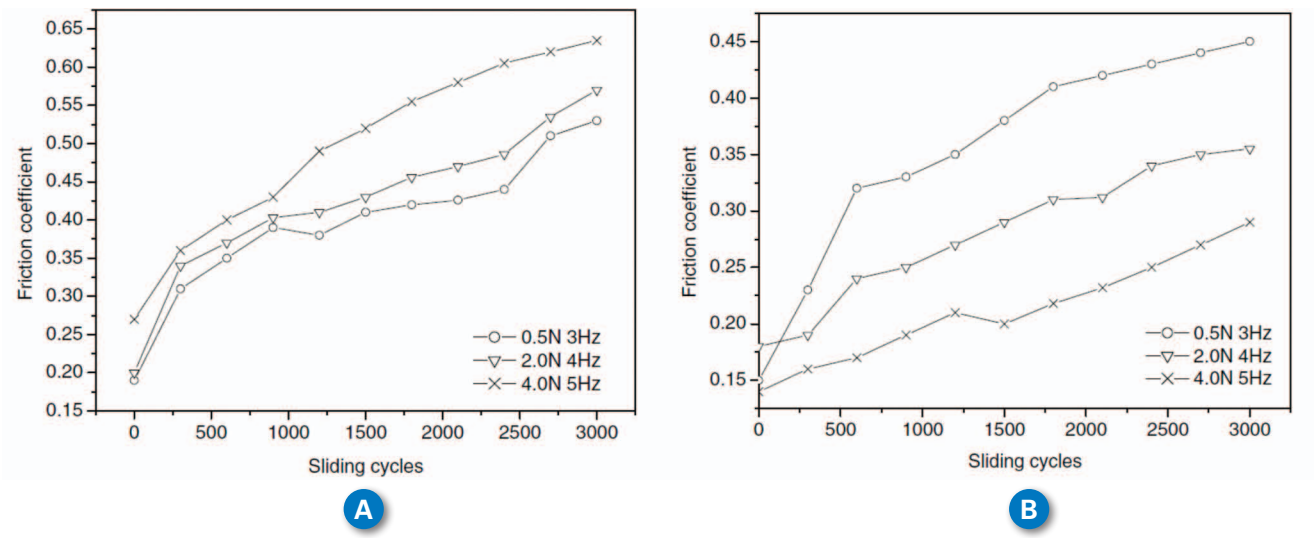

Figure 13. Friction coefficient of (a) Ni-Co and (b) Ni-Co-CNTs composite coatings/GCr15 steel ball as a function of sliding cycles.

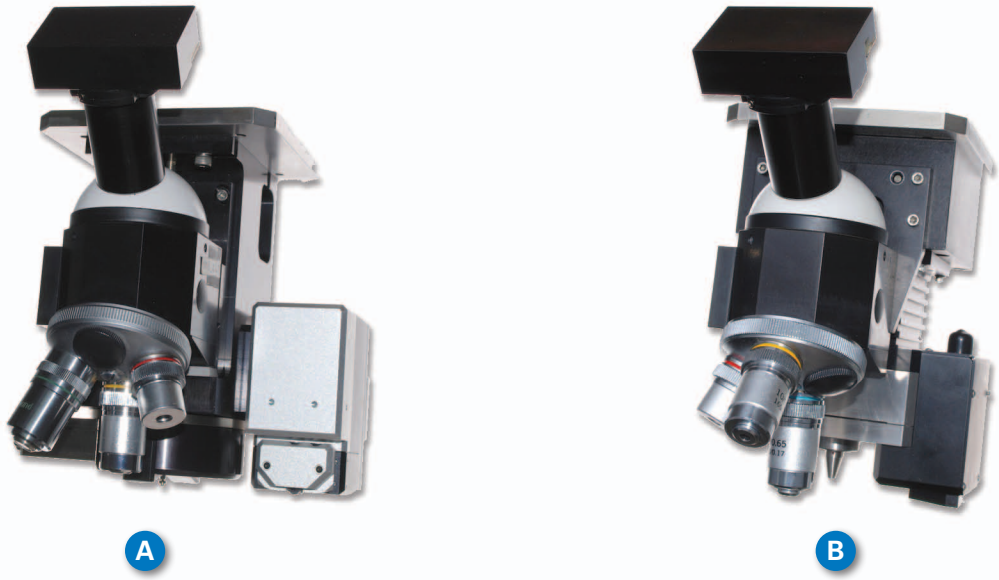

Figure 14. Nano-Module (a) and Micro-Module (b) for tribo-testers.

Table 4. List of ASTM scratch/indentation test standards.

ASTM #	Description
C1624-10	Adhesion Strength and Mechanical Failure Modes of Ceramic Coatings
D1474-98	Indentation Hardness of Organic Coatings
D1894-06	Static and Kinetic Coefficients of Friction of Plastic Film and Sheeting
D2240-00	Shore Hardness of Soft Materials
D4518-91	Static Friction of Coating Surfaces
D7027-05	Scratch Reistance of Polymeric Coatings and Plastics
D7187-05	Mechanistic Aspects of Scratch/Mar Behavior of Paint Coatings
E92-82 & E384-99	Vickers and Knoop Hardness Tests Using a Diamond Indenter
G171-03	Scratch Hardness of Materials Using a Diamond Stylus

References

1. N. Gitis, J. Xiao, A. Daugela, and A.K. Sikder. "Quantitative Nano & Micro Scale Metrology of Thin Films and Coatings" 4th International Conference on Industrial Tribology, (2004) 1-5.

2. A. Daugela, N. Gitis, and V. Gelfeinbein. "Phenomenological Nanoindentation Technique in Quality Control of Optoelectronics Devices," *Springer-Verlag*, (2008).

3. N. Gitis, I. Hermann, and S. Kuiry. "Nano and Micro Indentation and Scratch Tests of Mechanical Properties of Thin Films," 7th International Conference THE Coatings, (2008) 371-378.

4. N. Gitis, S. Kuiry, A. Daugela, M. Vinogradov, and J. Xiao. "Comprehensive Tribo-Mechanical Testing of Hard Coatings," *Society of Vacuum Coaters*, 505 (2006) 599-605.

5. M. Vinogradov, J. Xiao, and N. Gitis. "Scratch, Adhesion and Wear Testing of LCD Display Coatings," *The Adhesion Society*, (2004) 444-446.

6. X.B. Yan, T. Xu, S.R. Yang, H.W. Liu, and Q.J. Xue. "Characterization of Hydrogentated Diamond-Like Carbon Films Electrochemically Deposited on a Silicon Substrate," *Journal of Physics D: Applied Physics*, 37 (2004) 2416-2424.

7. L. Shi, C.F. Sun, P. Gao, F. Zhou, and W.M. Liu. "Electrodeposition. and Characterization of Ni-Co-Carbon Nanotubes Composite Coatings," *Elsevier*, 10.1016/j.surfcoat (2005).

Author

James Earle, Bruker Nano Surfaces Division
(james.earle@bruker-nano.com)

Dr. Suresh Kuiry, Bruker Nano Surfaces Division
(suresh.kuiry@bruker-nano.com)

Bruker Nano Surfaces Divison
Campbell, CA · USA
+1.408.376.4040/866.262.4040
productinfo@bruker-nano.com

www.bruker.com